Identification of key miRNAs and genes associated with stomach adenocarcinoma from The Cancer Genome Atlas database

Jixi Liu[1,†], Fang Liu[1,†], Yanfen Shi[2], Huangying Tan[3] and Lei Zhou[4]

1 Department of Gastroenterology, China-Japan Friendship Hospital, Beijing, China
2 Department of Pathology, China-Japan Friendship Hospital, Beijing, China
3 Department of Integrative Oncology, China-Japan Friendship Hospital, Beijing, China
4 Department of General Surgery, China-Japan Friendship Hospital, Beijing, China

Stomach adenocarcinoma (STAD) is the second leading cause of cancer death and a fuller understanding of its molecular basis is needed to develop new therapeutic targets. miRNA and mRNA data were downloaded from The Cancer Genome Atlas database, and the differentially expressed miRNAs and genes were identified. The target genes of differentially expressed miRNAs were screened by prediction tools. Furthermore, the biological function of these target genes was investigated. Several key miRNAs and their target genes were selected for validation using quantitative real-time polymerase chain reaction (qRT-PCR). The Gene Expression Omnibus (GEO) dataset was used to verify the expression of selected miRNAs and target genes. The diagnostic value of identified miRNAs and genes was accessed by receiver operating characteristic analysis. A total of 1248 differentially expressed genes were identified in STAD. Additionally, nine differentially expressed miRNAs were identified and 160 target genes of these nine miRNAs were identified via target gene detection. Interestingly, they were remarkably enriched in the calcium signaling pathway and bile secretion. qRT-PCR confirmed the expression of several key miRNAs and their target genes. The expression levels of hsa-miR-145-3p, hsa-miR-145-5p, *ADAM12*, *ACAN*, *HOXC11* and *MMP11* in the GEO database were compatible with the bioinformatics results. hsa-miR-139-5p, hsa-miR-145-3p and *MMP11* have a potential diagnostic value for STAD. Differential expression of the mature form of miRNAs (hsa-miR-139-5p, hsa-miR-145-3p, hsa-miR-145-5p and hsa-miR-490-3p) and genes including *ADAM12*, *ACAN*, *HOXC11* and *MMP11* and calcium and bile secretion signaling pathways may play important roles in the development of STAD.

Stomach carcinoma is a leading cause of cancer death [1]. Stomach adenocarcinoma (STAD) is the most common form of malignant stomach carcinoma and generally affects older people (50–70 years of age) [2].

According to the Lauren classification, there are two main types of STAD defined as the diffuse type and the intestinal type. Some risk factors are involved in STAD including smoking, high-salt diet, chronic gastritis and *Helicobacter pylori* infection [3]. Up to now, the principal treatment of STAD has been gastrectomy accompanied by chemotherapy and radiation therapy. Despite advances in the treatment of STAD, the 5-year survival rate is 5–15% [4]. Therefore, understanding the pathogenesis of STAD and searching for new therapeutic targets of STAD are urgent issues.

Recently, several studies have improved our understanding of the molecular mechanisms and signaling pathways underlying tumorigenesis in STAD. For example, some tyrosine kinase receptors, including ERBB2, EGFR, FGFR2 and MET, are activated, which leads to tumorigenesis in STAD [5]. Moreover, the phosphoinositide-3-kinase–Akt signaling pathway is activated and results in aggressive proliferation of STAD tumors [6–8].

The Cancer Genome Atlas (TCGA) database is an application platform for genome analysis consisting of large-sample genome sequencing data analysis for 33 types of cancers, including STAD [9]. miRNAs function as post-transcriptional regulators that can repress translation or promote degradation or cleavage of complementary target mRNA sequences [10], and moreover, miRNAs have emerged as key players in the pathogenesis of STAD [11]. In this study, we downloaded the miRNA and mRNA data for STAD from TCGA database and identified several differentially expressed miRNAs and a number of differentially expressed genes (DEGs). Then, we obtained the target genes of these differentially expressed miRNAs and analyzed their biological function. We used the quantitative real-time polymerase chain reaction (qRT-PCR) method to validate some bioinformatics analysis results. The Gene Expression Omnibus (GEO) was used to verify the expression of selected miRNAs and target genes. Finally, the diagnostic value of the identified miRNAs and genes was accessed by receiver operating characteristic (ROC) analysis. These findings may enable us to understand the progression and development of STAD.

Materials and methods

Identification of differentially expressed miRNAs and genes

From TCGA database (http://cancergenome.nih.gov), we downloaded miRNA (IlluminaHiSeq_miRNASeq) data of 84

samples (42 case samples and 42 normal samples) and mRNA (IlluminaHiSeq_RNASeqV2) data of 64 samples including 32 cases and 32 normal samples. Differential expression between normal and case samples was assessed using the R-bioconductor package DESEQ 2, and the *P*-value was calculated. Multiple hypothesis testing was performed via the Benjamini–Hochberg procedure. Differentially expressed miRNAs were screened with the threshold of the false discovery rate (FDR) < 0.001, log2 fold change > 2 and mean base > 100. The DEGs were screened with the threshold of FDR < 0.001 and absolute value of log2 fold change > 2.

Target gene detection of differentially expressed miRNAs

Six miRNA-target prediction tools including RNA22 (https://cm.jefferson.edu/rna22v2.0/), MIRANDA (http://www.microrna.org/), MIRDB (http://mirdb.org/miRDB/), MIRWALK (http://www.umm.uni-heidelberg.de/apps/zmf/mirwalk/index.html), PICTAR2 (http://pictar.mdc-berlin.de/) and TARGETSCAN (http://www.targetscan.org/) were utilized to predict target genes of differentially expressed miRNAs. Target genes predicted by more than four algorithms or verified by experiments provided by the miRWalk database were screened out. Finally, the regulatory network between differentially expressed miRNAs and target genes was established, which was visualized using CYTOSCAPE software [12].

Functional annotation of target genes

To further investigate the biological function, all DEGs and target genes of differentially expressed miRNAs were analyzed in the context of several databases such as Gene Ontology (GO) functional categories and the Kyoto Encyclopedia of Genes and Genomes (KEGG) biochemical

Table 1. The primer sequence in the qRT-PCR.

Primer	Sequence (5′ to 3′)
ADAM12	Forward: AAGACCTTGATACGACTGCTGTTT
	Reverse: GACTGGGGCTGAGGGACATT
ACAN	Forward: GTCACACCTGAGCAGCATCGT
	Reverse: CTGGTAGTCTTGGGCATTGTTGT
HOXC11	Forward: GGCTGAGGAGGAGAACACAAATC
	Reverse: GCCGCTTCTCTTTGTTGATATACAC
MMP11	Forward: CCCGCAACCGACAGAAGAG
	Reverse: GGCGTCACATCGCTCCATAC
18S rRNA	Forward: GTAACCCGTTGAACCCCATT
	Reverse: CCATCCAATCGGTAGTAGCG
hsa-miR-139-5p	Forward: TCTACAGTGCACGTGTCTCCAGT
hsa-miR-145-3p	Forward: GGATTCCTGGAAATACTGTTCT
hsa-miR-145-5p	Forward: GTCCAGTTTTCCCAGGAATC
hsa-miR-490-3p	Forward: CAACCTGGAGGACTCCATGCT
U6	Forward: CTCGCTTCGGCAGCACA
	Reverse: AACGCTTCACGAATTTGCGT

Table 2. The differentially expressed precursor form of miRNAs in STAD.

miRNA	Mean base	Log2 fold change	Standard error	Wald statistic	P	P adj	Up/down
hsa-mir-139	528.1534	−2.55383	0.202603	−12.6051	1.98×10^{-36}	3.51×10^{-34}	Down
hsa-mir-196a-1	392.8496	4.36323	0.345863	12.6155	1.73×10^{-36}	3.51×10^{-34}	Up
hsa-mir-196b	1049.324	4.091521	0.342584	11.94312	7.05×10^{-33}	8.35×10^{-31}	Up
hsa-mir-133a-1	900.0538	−3.34948	0.30633	−10.9342	7.91×10^{-28}	7.02×10^{-26}	Down
hsa-mir-1-2	1498.213	−3.23485	0.331376	−9.76188	1.64×10^{-22}	8.32×10^{-21}	Down
hsa-mir-145	48448.02	−2.37286	0.249126	−9.52473	1.65×10^{-21}	7.34×10^{-20}	Down
hsa-mir-135b	127.1043	2.927057	0.315644	9.273278	1.81×10^{-20}	6.41×10^{-19}	Up
hsa-mir-133b	127.2602	−2.76184	0.307681	−8.97632	2.80×10^{-19}	8.28×10^{-18}	Down
hsa-mir-490	255.5693	−3.83958	0.488705	−7.85665	3.95×10^{-15}	7.37×10^{-14}	Down

Table 3. Top 20 DEGs in STAD.

mRNA	Mean base	Log2 fold change	Standard error	Wald statistic	P	FDR	Up/down
CST1|1469	1950.411	7.706956	0.456963	16.86562	8.06×10^{-64}	1.56×10^{-59}	Up
COL10A1|1300	628.3591	6.468628	0.398018	16.25211	2.16×10^{-59}	2.09×10^{-55}	Up
ESM1|11082	164.0381	4.772024	0.307322	15.52774	2.25×10^{-54}	1.45×10^{-50}	Up
GABRD|2563	54.36653	3.639088	0.279383	13.02546	8.77×10^{-39}	4.24×10^{-35}	Up
HOXC10|3226	356.3751	6.328307	0.500079	12.65462	1.05×10^{-36}	4.08×10^{-33}	Up
COL11A1|1301	372.4826	5.984012	0.488973	12.23792	1.95×10^{-34}	6.28×10^{-31}	Up
MMP11|4320	2090.436	3.807886	0.314897	12.09247	1.16×10^{-33}	3.20×10^{-30}	Up
LYVE1|10894	921.3208	−3.57139	0.304514	−11.7282	9.14×10^{-32}	2.21×10^{-28}	Down
HOTAIR|100124700	45.54065	5.787221	0.502089	11.52628	9.73×10^{-31}	2.09×10^{-27}	Up
CTHRC1|115908	845.8077	3.275777	0.284703	11.50593	1.23×10^{-30}	2.38×10^{-27}	Up
LRFN4|78999	1583.359	2.39677	0.211807	11.3158	1.10×10^{-29}	1.93×10^{-26}	Up
C1QTNF6|114904	519.9666	2.003764	0.177663	11.27842	1.68×10^{-29}	2.70×10^{-26}	Up
PIWIL1|9271	134.2764	6.952432	0.621324	11.18971	4.58×10^{-29}	6.81×10^{-26}	Up
SH3GL2|6456	62.35987	−4.47119	0.407905	−10.9613	5.86×10^{-28}	8.09×10^{-25}	Down
CILP2|148113	126.4808	3.88935	0.356923	10.89688	1.19×10^{-27}	1.54×10^{-24}	Up
HOXC11|3227	157.2612	4.742368	0.449461	10.55122	5.01×10^{-26}	6.06×10^{-23}	Up
STRA6|64220	295.6888	4.633958	0.439962	10.53262	6.11×10^{-26}	6.95×10^{-23}	Up
ALPP|250	75.03801	6.927139	0.658164	10.52494	6.63×10^{-26}	7.12×10^{-23}	Up
CELSR3|1951	616.3266	2.799618	0.267519	10.46512	1.25×10^{-25}	1.27×10^{-22}	Up
MAPK15|225689	58.32309	3.731925	0.358736	10.40299	2.40×10^{-25}	2.32×10^{-22}	Up
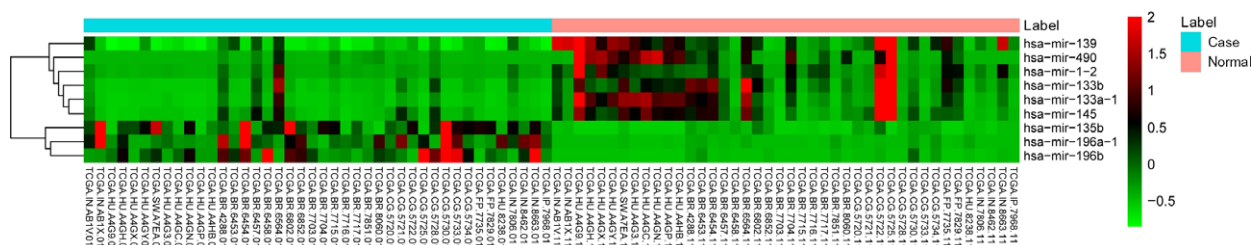
Fig. 1. Heat map of differentially expressed precursor form of miRNAs in STAD.

pathway using the Database for Annotation, Visualization and Integrated Discovery (DAVID).

qRT-PCR validation

Among the identified differentially expressed miRNAs and their target genes, we selected miRNAs and genes with expression significance for and association with STAD. Depending on this criterion, hsa-miR-139-5p, hsa-miR-145-3p, hsa-miR-145-5p, hsa-miR-490-3p and their target genes *ADAM12*, *ACAN*, *HOXC11* and *MMP11* were selected for validation. Three tumor tissues and three para-carcinoma tissues from participating individuals were obtained immediately after surgery. The collected tissues were frozen in

Fig. 2. Heat map of top 100 differentially expressed genes in STAD.

liquid nitrogen for further RNA extraction. All participating individuals provided informed consent with the approval of the China-Japan Friendship Hospital.

Total RNA of the tissue samples was extracted using the TRIzol® Reagent (Invitrogen, Carlsbad, CA, USA) according to the manufacturer's protocols. One microgram of RNA was applied to synthesize DNA by SuperScript® III Reverse Transcriptase (Invitrogen). Then real-time PCR was performed in an ABI 7500 real-time PCR system with SYBR® Green PCR Master Mix (Invitrogen). To confirm their reliability and validity, U6 and 18S rRNA were selected as the endogenous standards. All reactions were carried out in triplicate and relative gene expressions were analyzed by the $2^{-\Delta\Delta Ct}$ method. The primer sequence is shown in Table 1.

Validation of the expression of miRNAs and target genes by GEO

The GEO (http://www.ncbi.nlm.nih.gov/geo) database was used to validate the expression of selected miRNAs and targeted genes. We compared the expression levels of miRNAs and targeted genes between STAD cases and adjacent non-tumor controls and the difference of expression levels were displayed as box-plots.

ROC analyses

Using the PROC package in the R language we, performed the ROC analyses to assess the diagnostic value of selected miRNAs and target genes. The area under the curve (AUC) under binomial exact confidence interval was calculated and the ROC curve was generated.

Results

Differentially expressed miRNAs and genes

In this study, we found that nine miRNAs (three up-regulated and six down-regulated) and 1248 genes (371 up-regulated and 877 down-regulated) were differentially expressed in STAD. Table 2 shows all differentially expressed miRNAs (precursor form) including hsa-mir-139, hsa-mir-196a-1, hsa-mir-196b, hsa-mir-133a-1, hsa-mir-1-2, hsa-mir-145, hsa-mir-135b, hsa-mir-133b and hsa-mir-490. The top 20 DEGs are listed in Table 3. Additionally, heat maps of these differentially expressed precursor form of miRNAs and genes are shown in Figs 1 and 2, respectively.
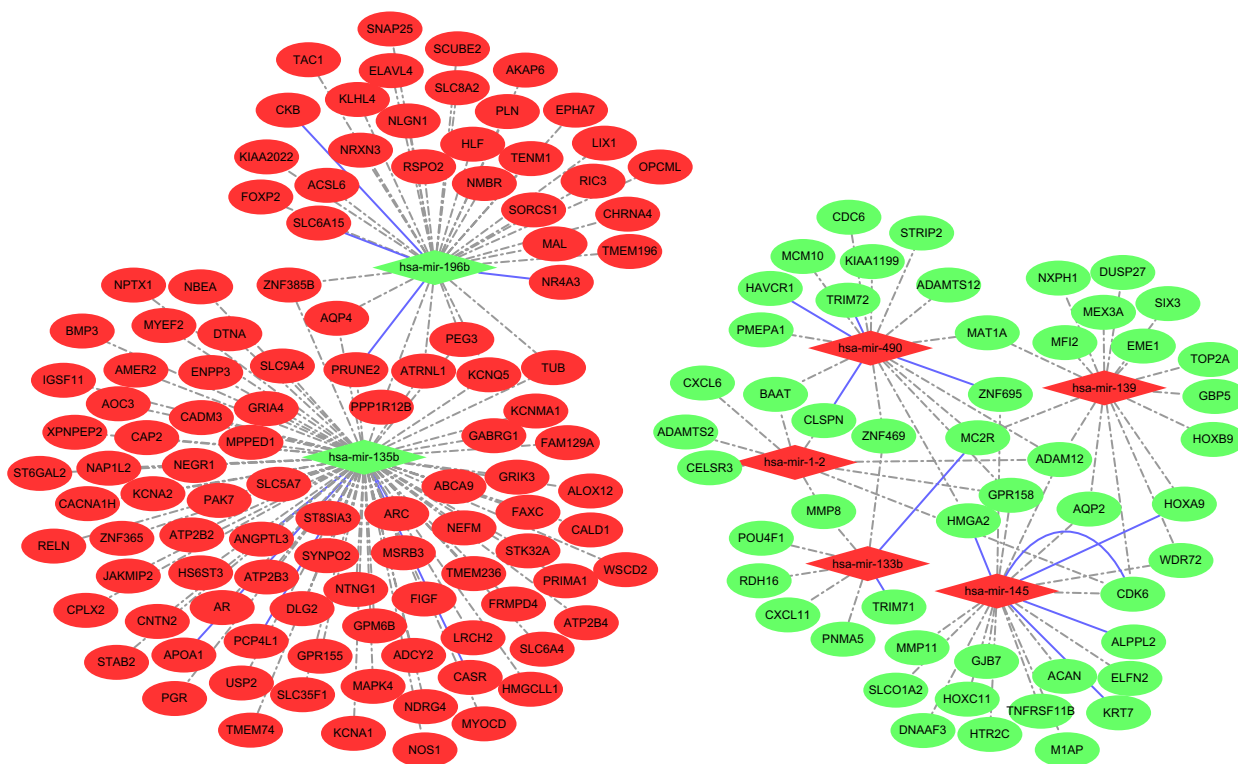
Fig. 3. Regulatory network of precursor form of miRNAs and target genes in STAD. Rhombus and oval represent miRNA and target gene, respectively. Red and green colors represent up-regulation and down-regulation, respectively. The full blue lines indicate the miRNA–mRNA validation pairs and the dashed lines indicate the miRNA–mRNA prediction pairs.

Table 4. GO function analysis of target genes.

Item	Item details	Count	P	FDR	Genes
Molecular function					
GO:0046872	Metal ion binding	37	3.36×10^{-9}	9.76×10^{-7}	ADCY2, MAT1A, MMP11, ALOX12, ATP2B3, TRIM72, XPNPEP2, MMP8, TRIM71, ATP2B4, ZNF469, EME1, KCNMA1, HMGCLL1, ADAMTS12, ADAM12, STK32A, NPTX1, ENPP3, FOXP2, NRXN3, PRUNE2, NOS1, MCM10, ALPPL2, ATP2B2, ZNF695, PGR, USP2, AR, NR4A3, ADAMTS2, ZNF385B, MSRB3, MFI2, MEX3A, RELN
GO:0005388	Calcium-transporting ATPase activity	3	7.23×10^{-6}	0.001048	ATP2B3, ATP2B4, ATP2B2
GO:0043565	Sequence-specific DNA binding (MF)	11	3.46×10^{-5}	0.002009	HLF, HOXA9, SIX3, HOXB9, FOXP2, HOXC11, POU4F1, PGR, TOP2A, AR, NR4A3
GO:0005516	Calmodulin binding	6	5.67×10^{-5}	0.002055	ATP2B3, ATP2B4, CALD1, NOS1, ATP2B2, SLC8A2
GO:0017022	Myosin binding	3	4.71×10^{-5}	0.002275	SLC6A4, CALD1, SNAP25
GO:0005216	Ion channel activity	7	3.15×10^{-5}	0.002282	GRIK3, KCNMA1, KCNQ5, GRIA4, GABRG1, CHRNA4, KCNA2
GO:0005515	Protein binding	38	5.65×10^{-5}	0.002341	CLSPN, DTNA, ACAN, ALOX12, HMGA2, SLC6A4, CELSR3, HOXA9, ATP2B4, HOXB9, EME1, KCNMA1, NTNG1, ADAM12, SORCS1, MYOCD, NEGR1, APOA1, MC2R, FRMPD4, CDC6, PLN, CASR, NOS1, MCM10, MAL, ZNF365, ATP2B2, PGR, TOP2A, USP2, AR, NEFM, MFI2, DLG2, KRT7, CDK6, SNAP25
GO:0017075	Syntaxin-1 binding	3	2.43×10^{-5}	0.002347	SLC6A4, CPLX2, SNAP25
GO:0004872	Receptor activity	19	7.64×10^{-5}	0.002463	CELSR3, HTR2C, HAVCR1, GRIK3, GPR158, MC2R, GRIA4, NMBR, NRXN3, CASR, EPHA7, TNFRSF11B, PGR, CHRNA4, AR, NR4A3, STAB 2, IGSF11, NLGN1
GO:0004222	Metalloendopeptidase activity	5	0.000108	0.00313	MMP11, MMP8, ADAMTS12, ADAM12, ADAMTS2
GO:0019899	Enzyme binding	6	0.000216	0.005705	APOA1, PGR, TOP2A, PRIMA1, AR, AKAP6
GO:0005249	Voltage-gated potassium channel activity	4	0.000312	0.006971	KCNMA1, KCNQ5, SNAP25, KCNA2
GO:0005372	Water transmembrane transporter activity	2	0.000295	0.00712	AQP2, AQP4
GO:0005244	Voltage-gated ion channel activity	5	0.000589	0.011389	CACNA1H, KCNMA1, KCNQ5, KCNA1, KCNA2
GO:0030165	PDZ domain binding	4	0.000562	0.011646	ATP2B4, AQP2, ATP2B2, DLG2
Biological process					
GO:0007268	Synaptic transmission	16	2.12×10^{-11}	1.60×10^{-8}	ADCY2, DTNA, HTR2C, GRIK3, TAC1, KCNMA1, KCNQ5, GRIA4, NPTX1, GABRG1, CHRNA4, DLG2, KCNA1, SLC5A7, SNAP25, KCNA2
GO:0055085	Transmembrane transport	18	5.43×10^{-10}	2.04×10^{-7}	ADCY2, ATP2B3, CACNA1H, ATP2B4, KCNMA1, KCNQ5, SLC6A15, SLC9A4, APOA1, SLCO1A2, AQP2, ATP2B2, AQP4, SLC8A2, KCNA1, SLC5A7, GPR155, KCNA2
GO:0006811	Ion transport	15	2.91×10^{-8}	7.29×10^{-6}	CACNA1H, GRIK3, KCNMA1, KCNQ5, SLC6A15, SLC9A4, GRIA4, GABRG1, SLCO1A2, CHRNA4, MFI2, SLC8A2, KCNA1, SLC5A7, KCNA2
GO:0007275	Multicellular organismal development	19	5.17×10^{-8}	9.73×10^{-6}	HLF, MMP11, HMGA2, CELSR3, HOXA9, SIX3, TRIM71, HOXB9, NTNG1, ARC, HOXC11, FIGF, NDRG4, EPHA7, POU4F1, GPM6B, ST6GAL2, RELN, BMP3
GO:0007155	Cell adhesion	13	1.45×10^{-6}	0.000218	OPCML, ACAN, CELSR3, ADAM12, NEGR1, CADM3, NRXN3, AOC3, STAB 2, IGSF11, CNTN2, RELN, NLGN1
GO:0030168	Platelet activation	8	1.12×10^{-5}	0.001409	ATP2B3, ATP2B4, KCNMA1, APOA1, FIGF, NOS1, ATP2B2, SLC8A2
GO:0007520	Myoblast fusion	3	1.41×10^{-5}	0.001517	CACNA1H, ADAM12, NOS1

Table 4. (Continued).

Item	Item details	Count	P	FDR	Genes
GO:0060748	Tertiary branching involved in mammary gland duct morphogenesis	2	5.94×10^{-5}	0.005596	PGR, AR
GO:0030574	Collagen catabolic process	3	9.46×10^{-5}	0.007122	MMP11, MMP8, ADAMTS2
GO:0006810	Transport	11	9.25×10^{-5}	0.007743	ATP2B3, CACNA1H, TRIM72, ATP2B4, GRIA4, NPTX1, SLC35F1, ATP2B2, AQP4, AR, ABCA9
GO:0007420	Brain development	6	0.000161	0.011038	CKB, SLC6A4, SIX3, EPHA7, ATP2B2, RELN
GO:0001503	Ossification	4	0.000198	0.011493	ACAN, MMP8, CASR, BMP3
GO:0051346	Negative regulation of hydrolase activity	2	0.000197	0.012361	APOA1, NOS1
GO:0030879	Mammary gland development	3	0.000265	0.01329	HOXA9, HOXB9, PGR
GO:0042391	Regulation of membrane potential	3	0.000265	0.01329	GRIK3, KCNMA1, CHRNA4
Cellular component					
GO:0005886	Plasma membrane	57	1.47×10^{-18}	2.16×10^{-16}	ADCY2, OPCML, DTNA, ATP2B3, FAM129A, SLC6A4, NBEA, CELSR3, HTR2C, XPNPEP2, GBP5, GRIK3, ATP2B4, PPP1R12B, TAC1, KCNMA1, KCNQ5, NTNG1, ACSL6, SLC6A15, SLC9A4, GPR158, ARC, ADAM12, NEGR1, CADM3, APOA1, MC2R, GRIA4, NMBR, CALD1, PMEPA1, CASR, EPHA7, ALPPL2, GABRG1, SLCO1A2, AQP2, ATP2B2, AOC3, PRIMA1, AQP4, CHRNA4, TUB, STAB 2, MFI2, IGSF11, GJB7, DLG2, SLC8A2, CNTN2, KCNA1, CAP2, SLC5A7, SNAP25, NLGN1, KCNA2
GO:0030425	Dendrite	12	4.11×10^{-11}	3.02×10^{-9}	ADCY2, GRIK3, NEGR1, GRIA4, CPLX2, EPHA7, ATP2B2, CHRNA4, AR, DLG2, RELN, NLGN1
GO:0016021	Integral to membrane	50	1.70×10^{-10}	8.34×10^{-9}	ADCY2, ATP2B3, CACNA1H, CELSR3, HTR2C, ELFN2, HAVCR1, GRIK3, KCNMA1, KCNQ5, ACSL6, SLC6A15, SLC9A4, GPR158, ADAM12, SORCS1, CADM3, GRIA4, PMEPA1, NRXN3, PLN, CASR, SLC35F1, GABRG1, SLCO1A2, AQP2, WSCD2, ATP2B2, TMEM74, AOC3, PRIMA1, ATRNL1, AQP4, CHRNA4, RIC3, GPM6B, ST8SIA3, RDH16, ST6GAL2, HS6ST3, IGSF11, GJB7, SLC8A2, KCNA1, ABCA9, SLC5A7, TMEM236, GPR155, KCNA2, TMEM196
GO:0043025	Neuronal cell body	12	3.15×10^{-10}	1.16×10^{-8}	TAC1, NEGR1, GRIA4, CALD1, CPLX2, EPHA7, ATP2B2, CHRNA4, DLG2, SLC8A2, CNTN2, SNAP25
GO:0045202	Synapse	12	7.76×10^{-9}	2.28×10^{-7}	DTNA, GRIK3, ARC, GRIA4, CPLX2, NOS1, GABRG1, PRIMA1, CHRNA4, DLG2, SNAP25, NLGN1
GO:0044224	Juxtaparanode region of axon	4	2.66×10^{-8}	6.51×10^{-7}	DLG2, CNTN2, KCNA1, KCNA2
GO:0045211	Postsynaptic membrane	8	1.06×10^{-6}	2.22×10^{-5}	GRIK3, ARC, GRIA4, EPHA7, GABRG1, CHRNA4, DLG2, NLGN1
GO:0008076	Voltage-gated potassium channel complex	6	3.53×10^{-6}	5.77×10^{-5}	KCNMA1, KCNQ5, CNTN2, KCNA1, SNAP25, KCNA2
GO:0005887	Integral to plasma membrane	17	3.34×10^{-6}	6.14×10^{-5}	OPCML, SLC6A4, GRIK3, ATP2B4, SLC6A15, MC2R, NMBR, ENPP3, NRXN3, CASR, EPHA7, MAL, AQP4, STAB 2, MFI2, CNTN2, NLGN1
GO:0016020	Membrane	38	6.88×10^{-6}	0.000101	ADCY2, CACNA1H, XPNPEP2, ELFN2, HAVCR1, KCNMA1, KCNQ5, SLC6A15, SORCS1, ENPP3, FIGF, NRXN3, PLN, SLC35F1, ALPPL2, SLCO1A2, AQP2, WSCD2, MAL, ATP2B2, TMEM74, ATRNL1, AQP4, CHRNA4, RIC3, GPM6B, ST8SIA3, RDH16, AKAP6, ST6GAL2, HS6ST3, SLC8A2, ABCA9, SLC5A7, TMEM236, GPR155, KCNA2, TMEM196

Table 4. (Continued).

Item	Item details	Count	P	FDR	Genes
GO:0030054	Cell junction	11	1.05×10^{-5}	0.00014	DTNA, GRIK3, ARC, GRIA4, GABRG1, PRIMA1, CHRNA4, GJB7, DLG2, SNAP25, NLGN1
GO:0031225	Anchored to membrane	6	1.17×10^{-5}	0.000144	OPCML, XPNPEP2, NEGR1, ALPPL2, MFI2, CNTN2
GO:0043197	Dendritic spine	5	1.50×10^{-5}	0.000169	ARC, FRMPD4, CALD1, NOS1, SLC8A2
GO:0005578	Proteinaceous extracellular matrix	7	4.58×10^{-5}	0.000481	ACAN, MMP11, MMP8, ADAMTS12, TNFRSF11B, ADAMTS2, RELN
GO:0005737	Cytoplasm	43	4.99×10^{-5}	0.000489	ADCY2, DTNA, CKB, KIAA1199, ALOX12, FAM129A, NBEA, HTR2C, HOXA9, TRIM71, PPP1R12B, BAAT, ARC, NMBR, CALD1, CDC6, FOXP2, HOXC11, NDRG4, SYNPO2, CPLX2, PRUNE2, NOS1, MCM10, AQP2, ZNF365, ATP2B2, PGR, TOP2A, AQP4, USP2, AR, TUB, PAK7, AKAP6, STAB 2, DLG2, MEX3A, KRT7, CDK6, SNAP25, RELN, KLHL4

Identification of miRNA–target interactions

In the present study, potential target genes of the differentially expressed precursor form of miRNAs were identified. We found 160 target genes with 270 miRNA–target pairs including 189 interaction pairs with miRNA up-regulated and target genes down-regulated and 81 interaction pairs with miRNA down-regulated and target genes up-regulated in STAD subjects. The established regulatory network of miRNA–targets is showed in Fig. 3. In addition, we further confirmed all of the miR–target interactions (MTIs) in TCGA data analysis using miRTarBAse. Our results showed that there was a total of 46 MTIs after the miRTarBAse analysis. However, we obtained a total of 187 MTIs by using the miR-Walk database. Therefore, the MTIs in the miRWalk database were more than those in the miRTarBAse database. Taking the intersection of the miRTarBAse and miRWalk databases, a total of 22 common MTIs was identified. The original MTIs from the miRWalk and miRTarBAse databases are listed in Tables S1 and S2, respectively. A Venn diagram of MTIs in the groups of the miRTarBAse database *vs* the miRWalk database is shown in Fig. S1.

Target genes enrichment analysis

Based on the DAVID database, we analyzed the biological function and pathways of these 160 target genes. Additionally, we also analyzed the function of all DEGs by KEGG. The enrichment of GO functional categories and KEGG biochemical pathways showed that these target genes were significantly enriched in calcium-transporting ATPase activity (FDR = 0.001048), calmodulin binding (FDR = 0.002055), calcium signaling pathway (FDR = 7.97×10^{-6}), salivary secretion (FDR = 9.13×10^{-5}), pancreatic secretion (FDR = 0.00209), neuroactive ligand–receptor interaction (FDR = 0.004133), cell adhesion molecules (FDR = 0.003932), bile secretion (FDR = 0.003801) and vascular smooth muscle contraction (FDR = 0.018674). A GO analysis of these enriched target genes is shown in Table 4, a KEGG pathway analysis of these target genes is listed in Table 5 and the pathway maps in KEGG of calcium signaling pathway and bile secretion are shown in Figs 4 and 5, which are related to STAD. Interestingly, all DEGs were found to be enriched in the signal pathway of gastric acid secretion (Fig. 6), which also plays a role in STAD.

qRT-PCR verification of selected miRNA and genes

To confirm the validity and reliability of bioinformatics results, we selected and assessed the expression levels of

Table 5. The KEGG pathway analysis of target genes.

| Item	Item details	Count	P	FDR	Genes
Kegg:04020	Calcium signaling pathway	9	1.03×10^{-7}	7.97×10^{-6}	*SLC8A2, ADCY2, ATP2B4, CACNA1H, HTR2C, ATP2B2, PLN, NOS1, ATP2B3*
Kegg:04970	Salivary secretion	6	2.37×10^{-6}	9.13×10^{-5}	*ADCY2, KCNMA1, ATP2B4, ATP2B2, NOS1, ATP2B3*
Kegg:04972	Pancreatic secretion	5	8.14×10^{-5}	0.00209	*ADCY2, KCNMA1, ATP2B4, ATP2B2, ATP2B3*
Kegg:04080	Neuroactive ligand–receptor interaction	7	0.000215	0.004133	*NMBR, MC2R, HTR2C, GABRG1, GRIK3, GRIA4, CHRNA4*
Kegg:04514	Cell adhesion molecules	5	0.000255	0.003932	*NRXN3, CNTN2, NLGN1, CADM3, NEGR1*
Kegg:04976	Bile secretion	4	0.000296	0.003801	*ADCY2, AQP4, SLCO1A2, BAAT*
Kegg:04270	Vascular smooth muscle contraction	4	0.001698	0.018674	*ADCY2, KCNMA1, CALD1, PPP1R12B*
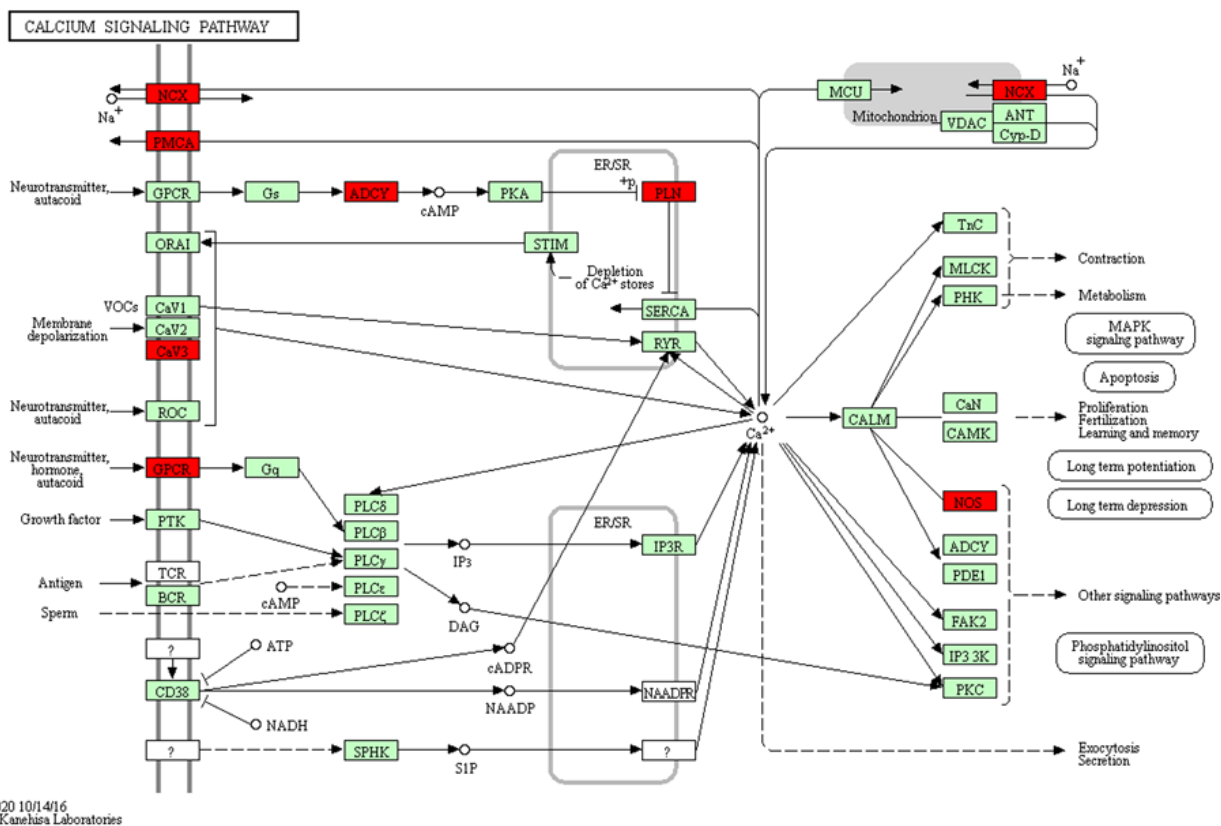
Fig. 4. Target genes that were significantly enriched in calcium signaling pathway. The red rectangles represent the target genes that are enriched in calcium signaling pathway. The figure was obtained by the Kanehisa Laboratories.

four key mature forms of miRNAs (hsa-miR-139-5p, hsa-miR-145-3p, hsa-miR-145-5p and hsa-miR-490-3p) and their target genes including *ADAM12*, *ACAN*, *HOXC11* and *MMP11* (Fig. 7). The results showed that hsa-miR-145-3p, hsa-miR-145-5p and hsa-miR-490-3p showed down-regulation, and their target genes (*ADAM12*, *ACAN*, *HOXC11* and *MMP11*) showed up-regulation, consistent with the bioinformatics results. However, the expression of hsa-miR-139-5p was inconsistent with the bioinformatics result.

Validation the expression of miRNAs and target genes

In this study, two down-regulated miRNAs (hsa-miR-145-3p and hsa-miR-145-5p) and four up-regulated target genes (*ADAM12*, *ACAN*, *HOXC11* and *MMP11*) in STAD were selected to perform the expression validation (Fig. 8). Different expression levels of them between STAD and non-tumor tissues were analyzed and depicted through box-plots. These
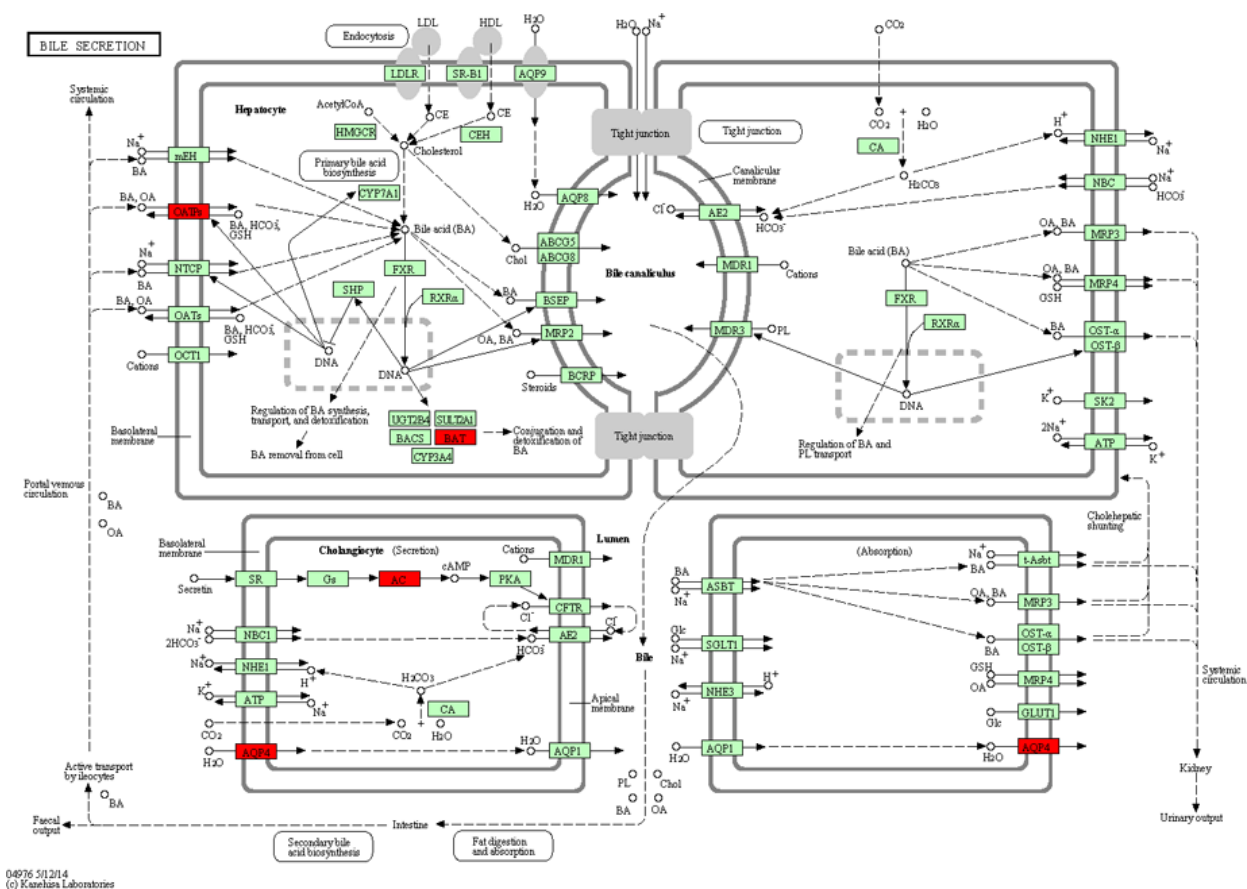
Fig. 5. Target genes that were significantly enriched in bile secretion. The red rectangles were represented the target genes that are enriched in bile secretion. The figure was obtained by the Kanehisa Laboratories.

box-plots were displayed visually by median and interquartile range. The expression levels of hsa-miR-145-3p and hsa-miR-145-5p were significantly down-regulated in the case group compared with the normal group and the expression of *ADAM12*, *ACAN*, *HOXC11* and *MMP11* was significantly up-regulated in the case group compared with the normal group. Compared with the normal group, the expression levels for the case group were consistent with our bioinformatics analysis.

ROC curve analysis

We performed ROC curve analyses and calculated the AUC to assess the discriminatory ability of two selected miRNAs (hsa-miR-139-5p and hsa-miR-145-3p) and one target gene (*MMP11*) from the GEO dataset (Fig. 9). The AUC for them was more than 0.7. *MMP11* had the largest AUC. For STAD diagnosis, the 1 – specificity (proportion of false positives) and sensitivity (proportion of true positives) of

hsa-miR-139-5p were 87.5% and 71.7%, respectively; the 1 – specificity (proportion of false positives) and sensitivity (proportion of true positives) of hsa-miR-145-3p were 100% and 56.7%, respectively; the 1 – specificity (proportion of false positives) and sensitivity (proportion of true positives) of *MMP11* were 100% and 83.3%, respectively.

Discussion

STAD remains the second leading cause of cancer death and makes up approximately 10% of newly diagnosed cancers [13]. Therefore, an understanding of the molecular mechanism of STAD is needed. In the current study, we obtained nine differentially expressed miRNAs and 1248 DEGs for STAD. Additionally, target gene detection revealed 160 target genes of these differentially expressed miRNAs. After biological function analysis, we found that these target genes were most significantly enriched in the calcium signaling pathway and bile secretion.
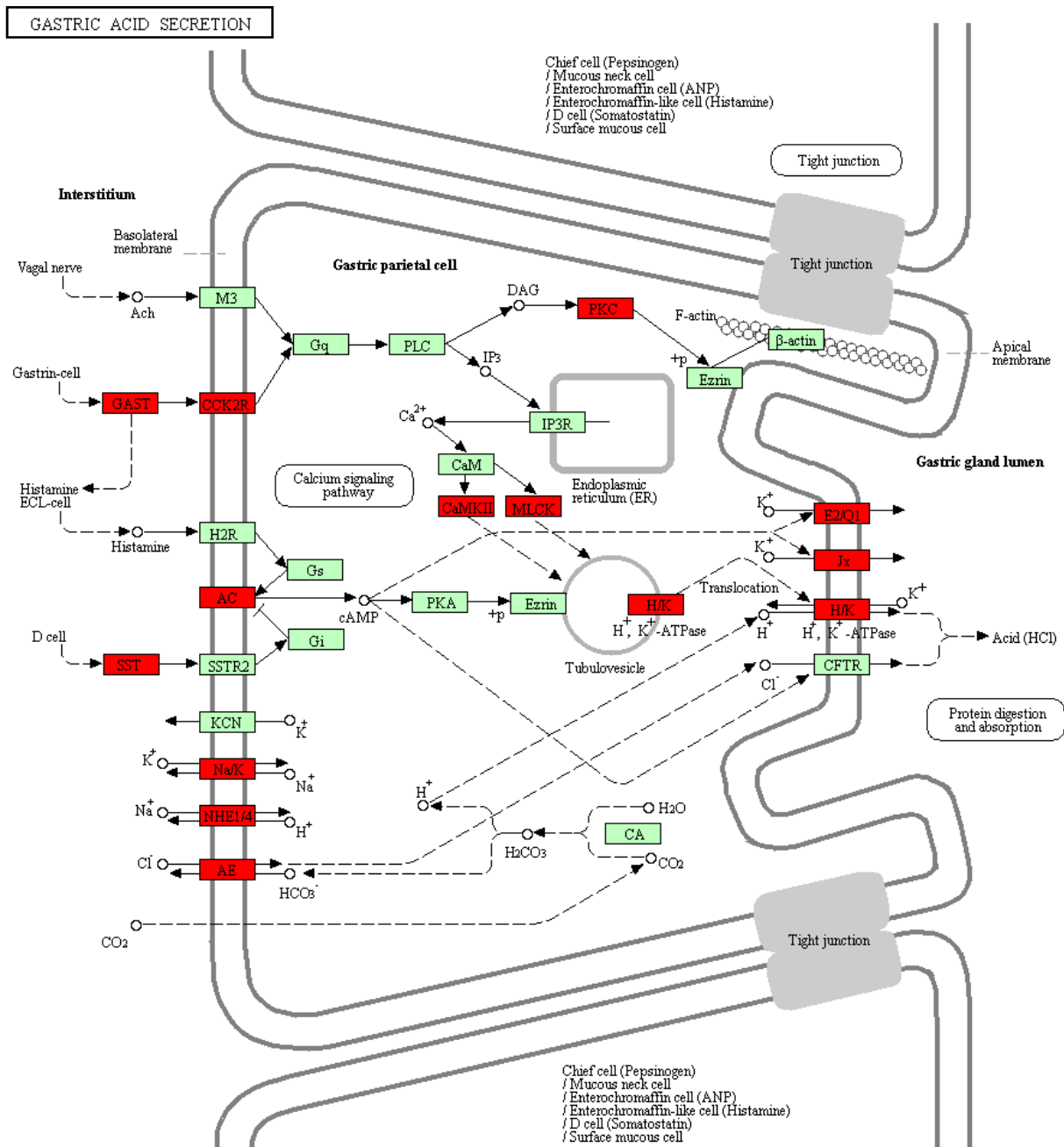
Fig. 6. Target genes that were significantly enriched in gastric acid secretion. The red rectangles represent the target genes that are enriched in gastric acid secretion. The figure was obtained by the Kanehisa Laboratories.

Calcium signals can regulate the majority of physiological processes ranging from cell proliferation to cell apoptosis [14]. It is reported that any disorders of Ca^{2+} channels and/or receptors will lead to various diseases, such as cancer [15]. In this study, we found that the target genes (*SLC8A2*, *ADCY2*, *ATP2B4*, *CACNA1H*, *HTR2C*, *ATP2B2*, *PLN*, *NOS1*

and *ATP2B3*) of differentially expressed miRNAs were associated with the calcium signaling pathway, which suggested a role for calcium signaling in STAD.

It is pointed out that there is a positive relationship between bile acid concentration and gastric carcinoma development, which suggests a carcinogenic role of bile
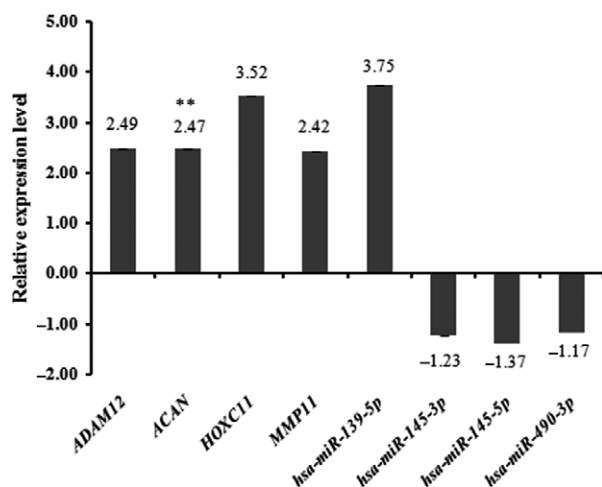
Fig. 7. Validation of differentially expressed mature forms of miRNAs and mRNAs in the STAD tissues by qRT-PCR. $**P < 0.01$.

acid in gastritis [16]. Furthermore, Suzuki *et al.* [17] also found that patients with a high level of bile acid developed gastric carcinoma more frequently than those patients with a low bile acid level. In this study, we found that target genes (*ADCY2*, *AQP4*, *SLCO1A2* and *BAAT*) were related to bile secretion, which suggested a relationship between bile secretion and STAD.

All in all, these identified target genes played roles in the biological processes of calcium signaling and bile secretion in STAD. Additionally, we also investigated the function of all DEGs by KEGG pathway analysis and found that these DEGs were remarkably involved in signaling pathways of gastric acid secretion.

The principal secretory function of the stomach is secreting gastric acid [18]. Gastric acid functions in a number of ways including modulating the gut microbiome, assisting in protein digestion and facilitating absorption of iron and calcium [19]. It is reported that *H. pylori* is related to gastric carcinoma [20]. Interestingly, it is found that in patients with relatives with gastric carcinoma, *H. pylori* infection is related to decreasing gastric acid secretion [21]. In this study, we found all DEGs were significantly enriched in the signaling pathway of gastric acid secretion, which further demonstrated the role of gastric acid secretion in the development of STAD.

Among identified miRNAs, mature the form of hsa-miR-139-5p, hsa-miR-145-3p, hsa-miR-145-5p and hsa-miR-490-3p was validated by qRT-PCR and the results were consistent with the bioinformatics results except for the expression of hsa-miR-139-5p. The small

sample size we used for qRT-PCR may account for this inconsistency. It is pointed out that hsa-miR-139-5p shows decreased expression associated with STAD [22,23]. Previous reports found that hsa-miR-145 was a potential tumor suppressor and hsa-miR-145-3p and hsa-miR-145-5p were down-regulated in stomach carcinoma [24–26]. Kuo *et al.* [22] demonstrated that hsa-miR-490-3p was down-regulated in STAD gastric carcinoma tissues. In this study, our results were in agreement with previous reports, which further demonstrated the role of these differentially expressed miRNAs in the process of STAD. Significantly, both hsa-miR-139-5p and hsa-miR-145-3p had a potential diagnostic value for STAD.

Additionally, we also validated the target genes (*ADAM12*, *ACAN*, *HOXC11* and *MMP11*) of these four miRNAs mentioned above, and their expression patterns were consistent with the bioinformatics results. ADAM12 is a complicated and multi-domain protein that functions in cell proliferation and movement [27]. Furthermore, it is strongly expressed in various cancers including stomach carcinoma [28,29]. That mutation of *ACAN* occurs in stomach carcinoma has been shown by comprehensive whole-genome and transcriptome sequencing analysis [30]. *HOXC11* is considered to be a novel potential oncogene with altered expression in stomach carcinoma pathogenesis by association analysis with candidate gene strategy [31]. *MMP11* is known a marker of tumor invasion and metastasis [32]. Moreover, previous reports detected the expression level of *MMP11* by microarray analysis and found that it was elevated in stomach carcinoma patients and quantitative polymerase chain reaction analysis also confirmed its up-regulated expression [32,33]. Herein, up-regulated expression of *ADAM12*, *ACAN*, *HOXC11* and *MMP11* may be involved in the pathology of STAD. Interestingly, *MMP11* was significantly associated with STAD diagnoses.

Besides the above validated differentially expressed miRNAs, we also found two miRNAs (hsa-miR-196b and hsa-miR-135b) were also differentially expressed in STAD. Moreover, hsa-miR-196 and hsa-miR-135 covered the most downstream target genes in the regulatory network between differentially expressed miRNAs and target genes. It has been demonstrated that the expression level of hsa-miR-196b is significantly higher in stomach carcinoma [34,35]. Additionally, overexpression of hsa-miR-196b is linked to stomach carcinoma and may be considered as a stomach carcinoma marker [36,37]. It was demonstrated that hsa-miR-135b is up-regulated in stomach carcinoma tissues [38,39].
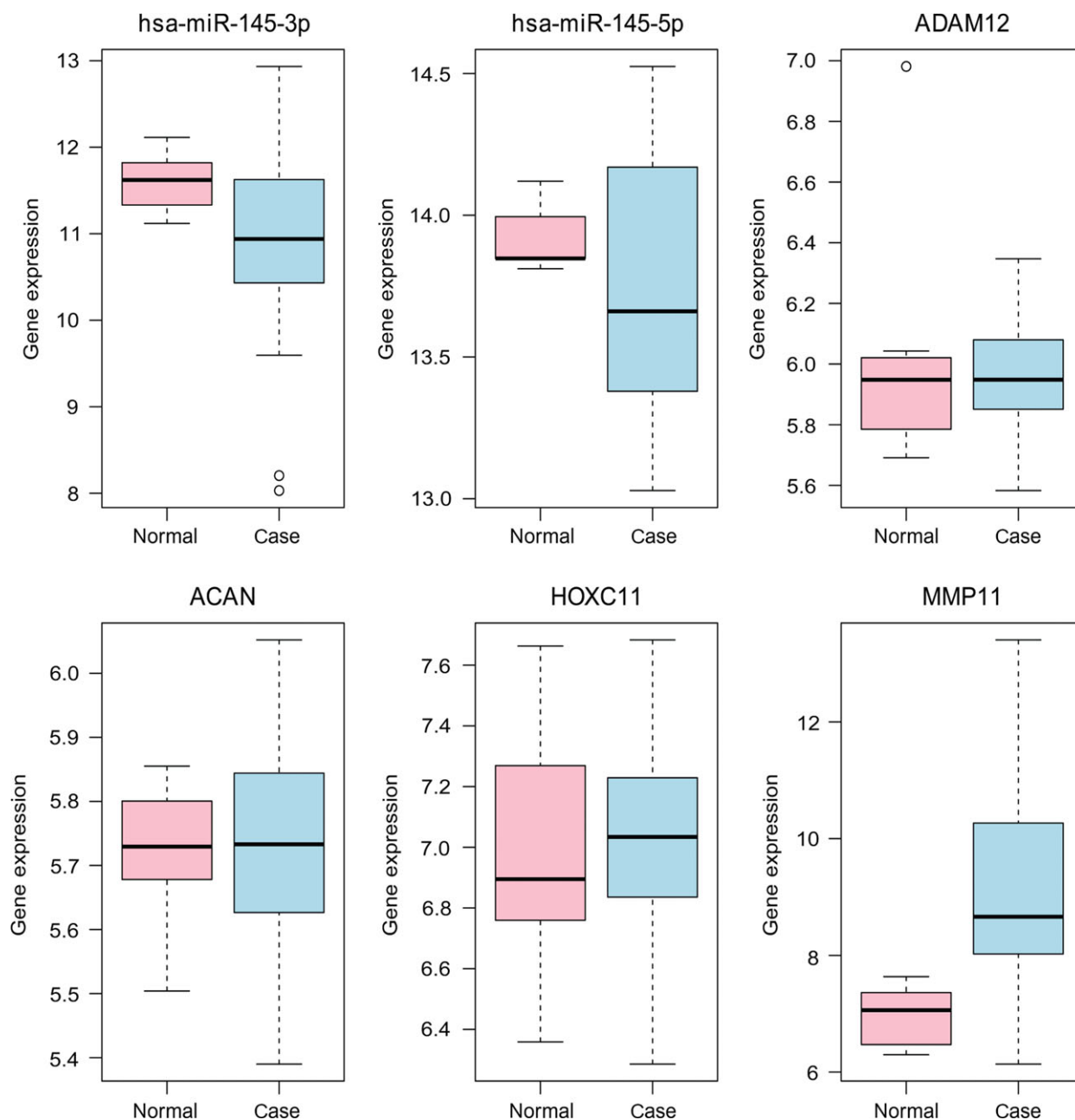
Fig. 8. Validation of the expression levels of selected miRNAs and in STAD based on GEO database. The x-axis shows the case and normal groups and the y-axis shows expression read counts. Case group and normal group indicate STAD tissues and adjacent non-tumor tissues.

Based on the results obtained in several studies, hsa-miR-135b is reported as a potential biomarker of the intestinal-type of STAD [40–43]. In our study, hsa-miR-196b and hsa-miR-135b were also up-regulated, which was in line with previous reports. Further qRT-PCR validation experiments for hsa-miR-196b and hsa-miR-135b are needed.

There are limitations to our study. Firstly, target site information for miRNA–mRNA pairs is needed for validation of the miRNA–mRNA interaction. Secondly, RNA-seq and miRNA-seq are further needed to screen larger numbers of candidate miRNA and mRNA. Thirdly, a luciferase assay for direct verification of the identified miRNA–target interactions is needed in further studies.
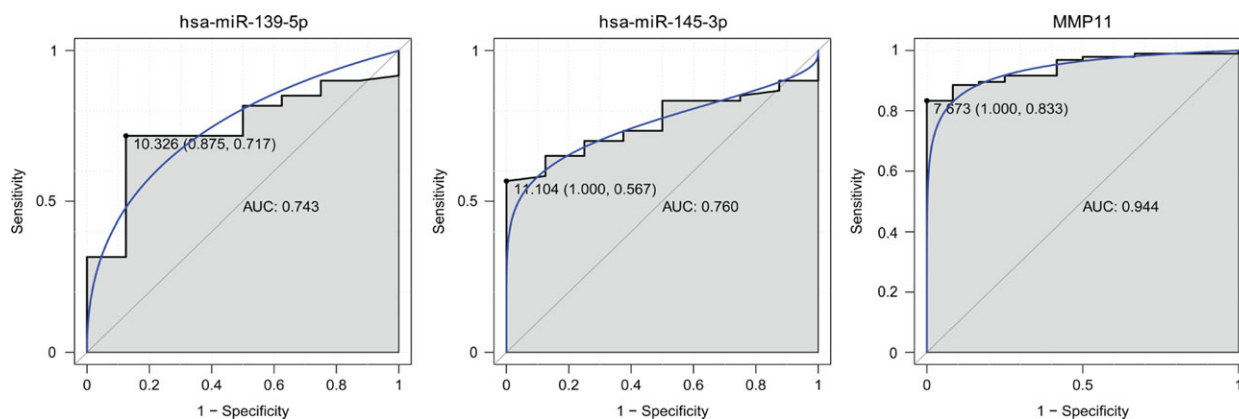
Fig. 9. ROC curves of selected miRNAs and target genes between STAD patients and healthy controls. The ROC curves were used to show the diagnostic ability of these selected miRNAs and target genes with 1 – specificity (the proportion of false positives) and sensitivity (the proportion of true positives). The *x*-axis shows 1 – specificity and the *y*-axis shows sensitivity.

Conclusions

All in all, we found four key differentially expressed miRNAs including hsa-miR-139-5p, hsa-miR-145-3p, hsa-miR-145-5p and hsa-miR-490-3p, four DEGs (*ADAM12*, *ACAN*, *HOXC11* and *MMP11*) and three related signaling pathways (calcium signaling pathway, bile secretion and gastric acid secretion) in STAD, which provide a novel field for understanding the pathological mechanism of STAD. In addition, hsa-miR-139-5p, hsa-miR-145-3p and *MMP11* have a potential diagnostic value for STAD.

Acknowledgements

Author contributions

The study was designed by LZ and HT; the grant receiver was LZ; the experiments were conducted by YS; the manuscript was written by JL and FL.

References

1 Kabel AM (2014) Jemal A, Bray F, Center MM, Ferlay J, Ward E, Forman D (2011): Global cancer statistics. *Cancer J Clinic* **61**, 69–90.

2 Kim BC, Jeong HO, Park D, Kim CH, Lee EK, Kim DH, Im E, Kim ND, Lee S and Yu BP (2014) Profiling age-related epigenetic markers of stomach adenocarcinoma in young and old subjects. *Cancer Inform* **14**, 47–54.

3 Lian G, Wei C, Wang D, Cui M, Wang Z, Liu X, Li W, Wang L, Wang Q and Zhang DY (2014) Protein profiling of *Helicobacter pylori*-associated gastric cancer. *Am J Pathol* **184**, 1343–1354.

4 Meireles SI, Cristo EB, Carvalho AF, Hirata R Jr, Pelosof A, Gomes LI, Martins WK, Begnami MD, Zitron C, Montagnini AL *et al.* (2004) Molecular classifiers for gastric cancer and nonmalignant diseases of the gastric mucosa. *Cancer Res* **64**, 1255–1265.

5 Bang YJ, Van Cutsem E, Feyereislova A, Chung HC, Shen L, Sawaki A, Lordick F, Ohtsu A, Omuro Y, Satoh T *et al.* (2010) Trastuzumab in combination with chemotherapy versus chemotherapy alone for treatment of HER2-positive advanced gastric or gastro-oesophageal junction cancer (ToGA): a phase 3, open-label, randomised controlled trial. *Lancet* **376**, 687–697.

6 Sawabu T, Seno H, Kawashima T, Fukuda A, Uenoyama Y, Kawada M, Kanda N, Sekikawa A, Fukui H, Yanagita M *et al.* (2007) Growth arrest-specific gene 6 and Axl signaling enhances gastric cancer cell survival via Akt pathway. *Mol Carcinog* **46**, 155–164.

7 Murakami D, Tsujitani S, Osaki T, Saito H, Katano K, Tatebe S and Ikeguchi M (2007) Expression of phosphorylated Akt (pAkt) in gastric carcinoma predicts prognosis and efficacy of chemotherapy. *Gastric Cancer* **10**, 45–51.

8 Kwon MJ and Nam TJ (2007) A polysaccharide of the marine alga *Capsosiphon fulvescens* induces apoptosis in AGS gastric cancer cells via an IGF-IR-mediated PI3K/Akt pathway. *Cell Biol Int* **31** (8), 768–775.

9 Lee H, Palm J, Grimes SM and Ji HP (2015) The Cancer Genome Atlas Clinical Explorer: a web and mobile interface for identifying clinical-genomic driver associations. *Genome Med* **7**, 112.

10 Bartel DP (2004) MicroRNAs: genomics, biogenesis, mechanism, and function. *Cell* **116**, 281–297.

11 Thiel A and Ristimaki A (2012) Gastric cancer: basic aspects. *Helicobacter* **17** (Suppl 1), 26–29.

12 Smoot ME, Ono K, Ruscheinski J, Wang PL and Ideker T (2011) Cytoscape 2.8: new features for data integration and network visualization. *Bioinformatics* **27**, 431–432.

13 Cunningham SC, Kamangar F, Kim MP, Hammoud S, Haque R, Iacobuzio-Donahue CA, Maitra A, Ashfaq R, Hustinx S, Heitmiller RE *et al.* (2006) Claudin-4, mitogen-activated protein kinase kinase 4, and stratifin are markers of gastric adenocarcinoma precursor lesions. *Cancer Epidemiol Biomarkers Prev* **15**, 281–287.

14 Carafoli E (2003) The calcium-signalling saga: tap water and protein crystals. *Nat Rev Mol Cell Biol* **4**, 326–332.

15 Elsholz F, Harteneck C, Muller W and Friedland K (2014) Calcium – a central regulator of keratinocyte differentiation in health and disease. *Eur J Dermatol* **24**, 650–661.

16 Tatsugami M, Ito M, Tanaka S, Yoshihara M, Matsui H, Haruma K and Chayama K (2012) Bile acid promotes intestinal metaplasia and gastric carcinogenesis. *Cancer Epidemiol Biomarkers Prev* **21**, 2101–2107.

17 Suzuki H, Hibi T and Marshall BJ (2007) *Helicobacter pylori*: present status and future prospects in Japan. *J Gastroenterol* **42**, 1–15.

18 Waldum HL, Kleveland PM and Fossmark R (2015) Upper gastrointestinal physiology and diseases. *Scand J Gastroenterol* **50**, 649–656.

19 Schubert ML (2016) Gastric acid secretion. *Curr Opin Gastroenterol* **32**, 452–460.

20 Bouvard V, Baan R, Straif K, Grosse Y, Secretan B, El Ghissassi F, Benbrahim-Tallaa L, Guha N, Freeman C, Galichet L *et al.* (2009) A review of human carcinogens–Part B: biological agents. *Lancet Oncol* **10**, 321–322.

21 Vilkin A, Levi Z, Morgenstern S, Shmuely H, Gal E, Hadad B, Hardi B and Niv Y (2008) Higher gastric mucin secretion and lower gastric acid output in first-degree relatives of gastric cancer patients. *J Clin Gastroenterol* **42**, 36–41.

22 Kuo WT, Su MW, Lee YL, Chen CH, Wu CW, Fang WL, Huang KH and Lin WC (2015) Bioinformatic interrogation of 5p-arm and 3p-arm specific miRNA expression using TCGA datasets. *J Clin Med* **4**, 1798–1814.

23 Guo J, Miao Y, Xiao B, Huan R, Jiang Z, Meng D and Wang Y (2009) Differential expression of microRNA species in human gastric cancer versus non-tumorous tissues. *J Gastroenterol Hepatol* **24**, 652–657.

24 Saito Y, Suzuki H and Hibi T (2009) The role of microRNAs in gastrointestinal cancers. *J Gastroenterol* **44** (Suppl 19), 18–22.

25 Kent OA and Mendell JT (2006) A small piece in the cancer puzzle: microRNAs as tumor suppressors and oncogenes. *Oncogene* **25**, 6188–6196.

26 Chen Z, Liu X, Hu Z, Wang Y, Liu M, Liu X, Li H, Ji R, Guo Q and Zhou Y (2015) Identification and characterization of tumor suppressor and oncogenic miRNAs in gastric cancer. *Oncol Lett* **10**, 329–336.

27 Shao S, Li Z, Gao W, Yu G, Liu D and Pan F (2014) ADAM-12 as a diagnostic marker for the proliferation, migration and invasion in patients with small cell lung cancer. *PLoS ONE* **9**, e85936.

28 Iba K, Albrechtsen R, Gilpin BJ, Loechel F and Wewer UM (1999) Cysteine-rich domain of human ADAM 12 (meltrin alpha) supports tumor cell adhesion. *Am J Pathol* **154**, 1489–1501.

29 Carl-McGrath S, Lendeckel U, Ebert M, Roessner A and Rocken C (2005) The disintegrin-metalloproteinases ADAM9, ADAM12, and ADAM15 are upregulated in gastric cancer. *Int J Oncol* **26**, 17–24.

30 Zhang J, Huang JY, Chen YN, Yuan F, Zhang H, Yan FH, Wang MJ, Wang G, Su M, Lu G *et al.* (2015) Whole genome and transcriptome sequencing of matched primary and peritoneal metastatic gastric carcinoma. *Sci Rep* **5**, 13750.

31 Du M, Wang W, Jin H, Wang Q, Ge Y, Lu J, Ma G, Chu H, Tong N, Zhu H *et al.* (2015) The association analysis of lncRNA HOTAIR genetic variants and gastric cancer risk in a Chinese population. *Oncotarget* **6**, 31255–31262.

32 Shin NR, Jeong EH, Choi CI, Moon HJ, Kwon CH, Chu IS, Kim GH, Jeon TY, Kim DH, Lee JH *et al.* (2012) Overexpression of Snail is associated with lymph node metastasis and poor prognosis in patients with gastric cancer. *BMC Cancer* **12**, 521.

33 Xu J, E C, Yao Y, Ren S, Wang G and Jin H (2016) Matrix metalloproteinase expression and molecular interaction network analysis in gastric cancer. *Oncol Lett* **12**, 2403–2408.

34 Liao YL, Hu LY, Tsai KW, Wu CW, Chan WC, Li SC, Lai CH, Ho MR, Fang WL, Huang KH *et al.* (2012) Transcriptional regulation of miR-196b by ETS2 in gastric cancer cells. *Carcinogenesis* **33**, 760–769.

35 Yang Q, Zhang RW, Sui PC, He HT and Ding L (2015) Dysregulation of non-coding RNAs in gastric cancer. *World J Gastroenterol* **21**, 10956–10981.

36 Popovic R, Riesbeck LE, Velu CS, Chaubey A, Zhang J, Achille NJ, Erfurth FE, Eaton K, Lu J, Grimes HL *et al.* (2009) Regulation of mir-196b by MLL and its overexpression by MLL fusions contributes to immortalization. *Blood* **113**, 3314–3322.

37 Tsai KW, Hu LY, Wu CW, Li SC, Lai CH, Kao HW, Fang WL and Lin WC (2010) Epigenetic regulation of miR-196b expression in gastric cancer. *Genes Chromosom Cancer* **49**, 969–980.

38 Wang M, Gu H, Wang S, Qian H, Zhu W, Zhang L, Zhao C, Tao Y and Xu W (2012) Circulating miR-17-5p and miR-20a: molecular markers for gastric cancer. *Mol Med Rep* **5**, 1514–1520.

39 Shrestha S, Hsu SD, Huang WY, Huang HY, Chen W, Weng SL and Huang HD (2014) A systematic review of microRNA expression profiling studies in human gastric cancer. *Cancer Med* **3**, 878–888.

40 Ribeiro-dos-Santos A, Khayat AS, Silva A, Alencar DO, Lobato J, Luz L, Pinheiro DG, Varuzza L, Assumpcao M, Assumpcao P *et al.* (2010) Ultra-deep sequencing reveals the microRNA expression pattern of the human stomach. *PLoS ONE* **5**, e13205.

41 Moreira FC, Assumpcao M, Hamoy IG, Darnet S, Burbano R, Khayat A, Goncalves AN, Alencar DO, Cruz A, Magalhaes L *et al.* (2014) MiRNA expression profile for the human gastric antrum region using ultra-deep sequencing. *PLoS ONE* **9**, e92300.

42 Gomes LL, Moreira FC, Hamoy IG, Santos S, Assumpcao P, Santana AL and Ribeiro-Dos-Santos A (2014) Identification of miRNAs expression profile in gastric cancer using self-organizing maps (SOM). *Bioinformation* **10**, 246–250.

43 Darnet S, Moreira FC, Hamoy IG, Burbano R, Khayat A, Cruz A, Magalhaes L, Silva A, Santos S, Demachki S *et al.* (2015) High-throughput sequencing of miRNAs reveals a tissue signature in gastric cancer and suggests novel potential biomarkers. *Bioinform Biol Insights* **9** (Suppl 1), 1–8.

Supporting information

Additional Supporting Information may be found online in the supporting information tab for this article:

Fig. S1. Venn diagram of MTIs in the groups of miR-TarBAse database *vs* miRWalk database.

Table S1. The original miR–target interactions from the miRWalk database.

Table S2. The original miR–target interactions from the miRTarBAse database.